The Plant Cell, Vol. 8, 155–168, February 1996 © 1996 American Society of Plant Physiologists

AINTEGUMENTA, an *APETALA2*-like Gene of Arabidopsis with Pleiotropic Roles in Ovule Development and Floral Organ Growth

Robert C. Elliott,[a] Andreas S. Betzner,[b] Eric Huttner,[b] Marie P. Oakes,[b] William Q. J. Tucker,[b] Denise Gerentes,[c] Pascual Perez,[c] and David R. Smyth[a,1]

[a] Department of Genetics and Developmental Biology, Monash University, Clayton, Victoria 3168, Australia
[b] Groupe Limagrain Pacific Pty. Ltd., Biocem Pacific Laboratory, Research School of Biological Sciences, Australian National University, GPO Box 475, Canberra, ACT 2601, Australia
[c] Biocem Laboratoire de Biologie Cellulaire et Moleculaire, Campus Universitaire des Cézeaux 24, Av. des Landais, 63170 Aubière, France

To understand better the role of genes in controlling ovule development, a female-sterile mutant, *aintegumenta* (*ant*), was isolated from Arabidopsis. In ovules of this mutant, integuments do not develop and megasporogenesis is blocked at the tetrad stage. As a pleiotropic effect, narrower floral organs arise in reduced numbers. More complete loss of floral organs occurs when the *ant* mutant is combined with the floral homeotic mutant *apetala2*, suggesting that the two genes share functions in initiating floral organ development. The *ANT* gene was cloned by transposon tagging, and sequence analysis showed that it is a member of the *APETALA2*-like family of transcription factor genes. The expression pattern of *ANT* in floral and vegetative tissues indicates that it is involved not only in the initiation of integuments but also in the initiation and early growth of all primordia except roots.

INTRODUCTION

Ovule development involves four main events: (1) initiation of primordia; (2) regionalization of the primordia into three zones, the stalk (funiculus), a central region (chalaza), and the tip (nucellus); (3) initiation, growth, and differentiation of the enveloping integument(s) from the chalazal region; and (4) development of the embryo sac from a nucellus-derived megaspore mother cell (Bouman, 1984; Reiser and Fischer, 1993).

As an approach to understanding ovule development, mutants that affect a range of different developmental aspects have been obtained in Arabidopsis. Development of the wild-type ovule has been described in detail for this species (Robinson-Beers et al., 1992; Modrusan et al., 1994; Schneitz et al., 1995). Most mutations reported to date involve disruptions to the integuments. These mutations reduce their size (e.g., *short integuments* [*sin*]; Robinson-Beers et al., 1992; Lang et al., 1994), result in excessive, region-specific integument growth (*superman* [*sup*]; Gaiser et al., 1995), convert their identity (*bell* [*bel*]; Modrusan et al., 1994; Ray et al., 1994), or affect late integument differentiation into the seed coat (*apetala2* [*ap2*]; Jofuku et al., 1994; and *aberrant testa shape* [*ats*]; Léon-Kloosterziel et al., 1994). General conclusions from these studies have been limited thus far. However, it seems clear that integument and embryo sac development are interdependent processes because none of the mutants that severely disrupt integuments generate a normal embryo sac (Reiser and Fischer, 1993).

Ovule development genes may also play parallel roles earlier in flower development. For example, the *AGAMOUS* (*AG*) gene, whose expression in integuments is suppressed by *BEL*, is involved in specifying floral organ identity (Bowman et al., 1989; Weigel and Meyerowitz, 1994). *AG* may also have an identity function in ovules, because a change in integument identity is the consequence of ectopic expression of *AG* within them (Modrusan et al., 1994; Ray et al., 1994). The *SUP* gene is also expressed in developing flowers as well as in ovules. In flowers, it plays a role in maintaining the stamen/carpel boundary, and this may occur through a growth-suppressing function parallel to its proposed action in the developing integuments (Sakai et al., 1995). As a final example, the *AP2* gene is also involved in the development of both ovules and floral organs. In floral organs, it controls the identity of the first two whorls as well as playing a cadastral role in spatially restricting the expression of another organ identity gene, *AG* (Drews et al., 1991). Control of *AG* activity may also be a role of *AP2* in early ovule development, although independent of the later regulation of *AG* by *BEL* (Modrusan et al., 1994).

[1] To whom correspondence should be addressed.

Thus, to understand better the mechanisms of ovule development, it is important to obtain additional mutant genes in new classes. It may be that such genes will also throw light on earlier aspects of flower development through their common involvement in both. To this end, we isolated a female-sterile mutant (*aintegumenta* [*ant*]) that shows severe disruptions in ovule development. The mutant also results in defects outside the ovule in all four whorls of the flower. The *ANT* gene was cloned by transposon tagging, revealing that it is related to the floral homeotic gene *AP2*. By analyzing its expression pattern in wild-type tissues in relation to the mutant phenotype, we propose that *ANT* plays a specific role in initiating integument growth in Arabidopsis ovules and a general role in initiating and maintaining early floral primordium growth.

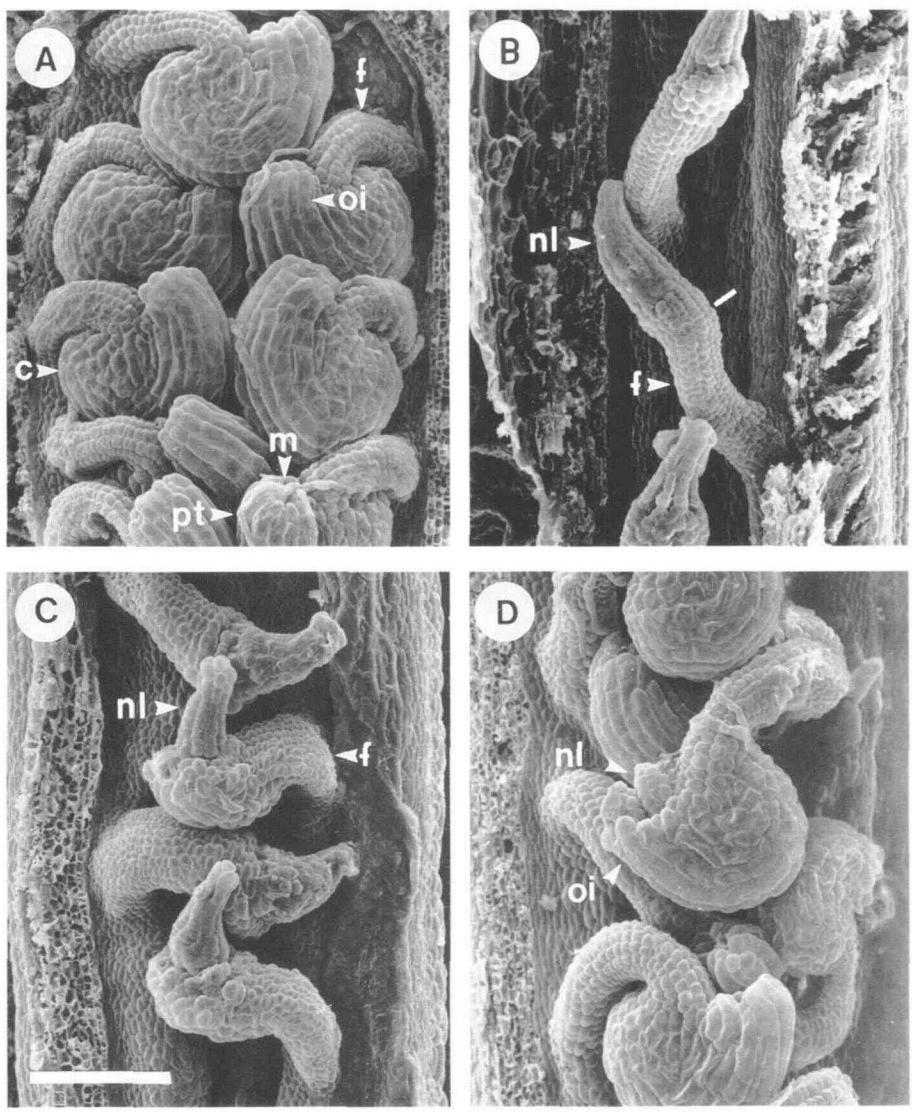

Figure 1. Scanning Electron Microscopy of Mature Ovules of Wild-Type and *ant-9* Strains of Arabidopsis.

A valve has been dissected from the gynoecium to reveal underlying ovules in each instance.

(A) Landsberg *erecta* wild type.

(B) *ant-9* mutant in a C24 background. Integuments are absent, and the site where they normally arise is indicated (white line).

(C) *ant-9* mutant in a Landsberg *erecta* background. The ovule defects are slightly less severe.

(D) *ant-9* mutant complemented with a transgenic *ANT* gene.

c, chalaza; f, funiculus; m, micropyle; nl, nucellus-like structure; oi, outer integument; pt, pollen tube. Bar in **(C)** = 50 μm for **(A)** to **(D)**.

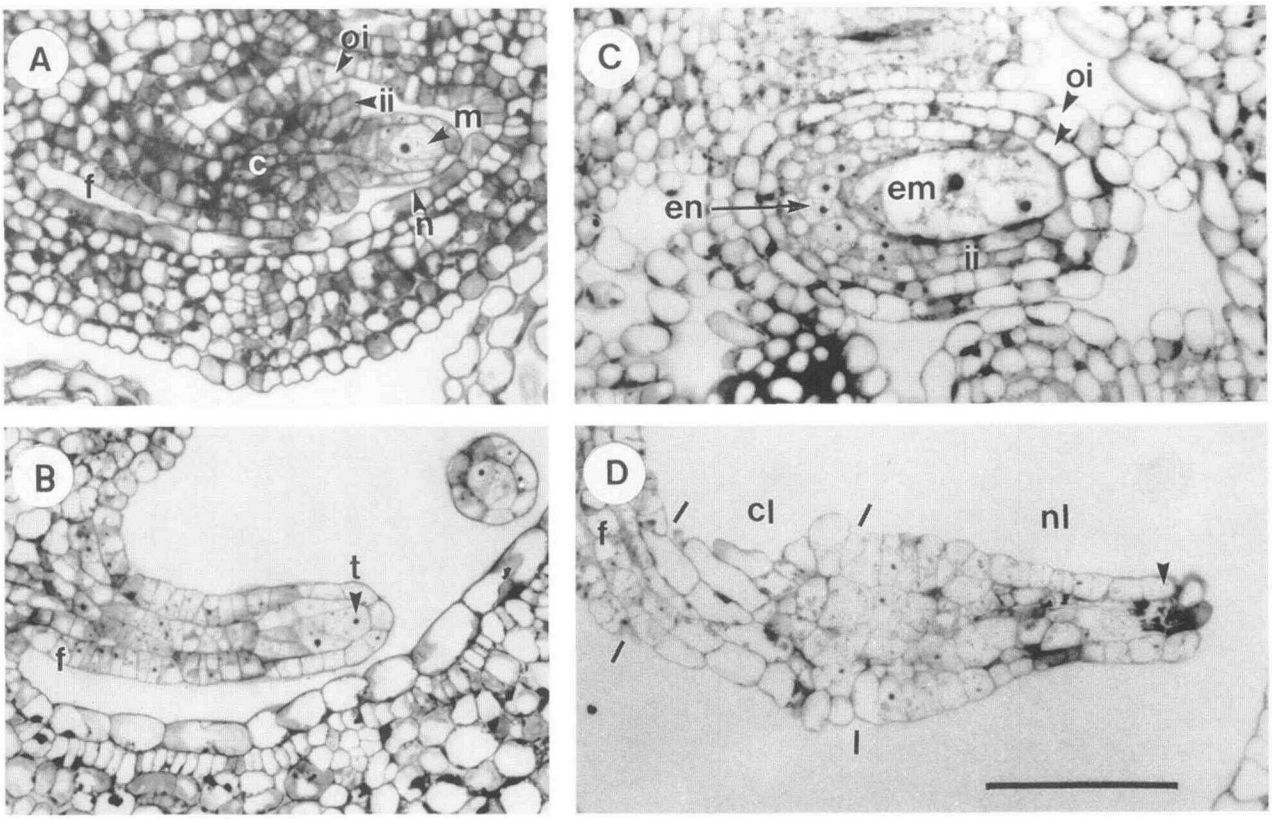

Figure 2. Sections of Wild-Type and *ant-9* Ovules at Two Stages of Development.

All plants had a Landsberg *erecta* background.

(A) Wild-type ovule at the stage when integument growth has commenced and the megaspore has just been generated.

(B) *ant-9* ovule at the same age as the ovule shown in **(A)**. Integument initiation does not occur in the *ant-9* ovule, but normal megasporogenesis apparently occurs to the tetrad stage.

(C) Wild-type ovule at maturity when the embryo sac is embedded in a two-layered outer integument and a three-layered inner integument, with the two inner layers having differentiated into the endothelium in the basal (chalazal) region. The micropyle lies to the right but is not present in this section.

(D) *ant-9* ovule at the same age as the ovule shown in **(C)**. The ovule's nucellus-like region at the apex contains collapsed, darkly staining cells (arrowhead), and there is no sign of an embryo sac. A collar of larger, bulbous epidermal cells usually occurs in the central, chalaza-like region where the integuments would normally have arisen, although they mostly lie outside the plane of this section. The stalk (funiculus) is relatively normal. Lines indicate the limits of the three regions.

c, chalaza; cl, chalaza-like region; em, embryo sac; en, endodermis; f, funiculus; ii, inner integument; m, megaspore; n, nucellus; nl, nucellus-like region; oi, outer integument; t, tetrad. Bar in **(D)** = 50 μm for **(A)** to **(D)**.

RESULTS

Ovule Development Is Abnormal in *ant-9* Mutants

As illustrated in Figure 1, female sterility in *ant-9* mutants is a consequence of major disruptions to ovule development. The mature ovules lack integuments, and the nucellus develops as a thin, elongated structure, whereas the stalk (funiculus) is relatively unaffected (compare Figures 1B and 1A). The number of ovules per flower is reduced by more than half (15.0 ± 0.8 per flower on average, compared with 39.9 ± 1.1 in wild-type flowers). This cannot be due to a smaller gynoecium because the ovules that do arise are more distantly spaced than in the wild type.

Developmental studies illustrated in Figure 2 show that integument growth is not initiated in *ant-9* mutant ovules. The two integuments normally arise as ringlike epidermal swellings on the fingerlike primordia. Anticlinal divisions in these rings then generate two sheaths of tissue (Figure 2A) that eventually encase the nucellus (Figure 2C). In *ant-9* mutants, the epidermis of this region remains flat (Figure 2B).

The other major effect of the *ant-9* mutation on ovule development is a block to embryo sac formation. In wild-type primordia, the nucellus normally differentiates into the megaspore mother cell and an enveloping epidermis just before the

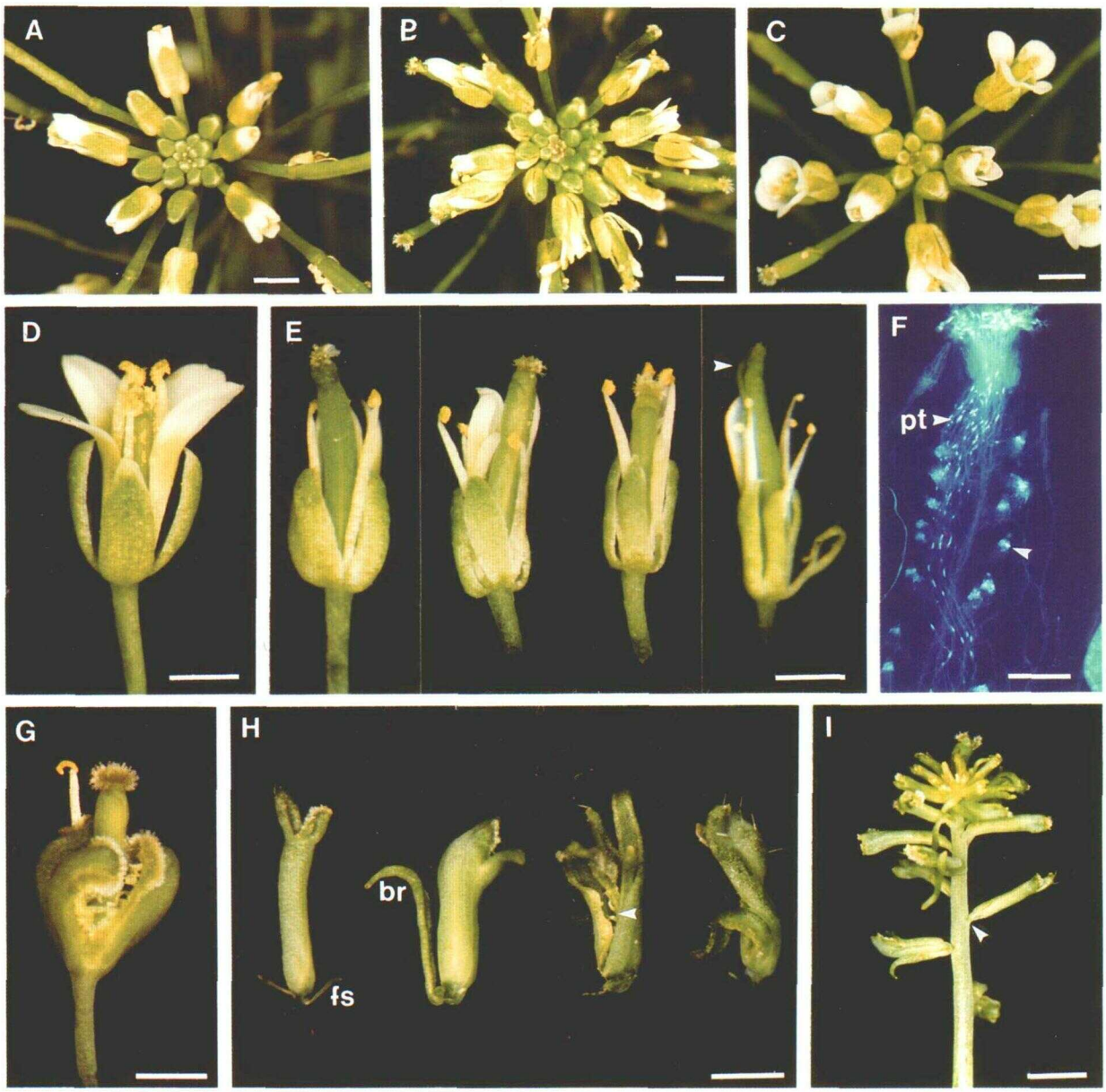

Figure 3. Morphology of *ant-9* Single and *ant-9 ap2-2* Double Mutant Flowers.

All flowers are in the Landsberg *erecta* background except for the rightmost flower in **(E)**.

(A) to **(C)** Vertical views of inflorescences of the Landsberg *erecta* wild type, an *ant-9* plant, and *ant-9* complemented with a transgenic copy of the wild-type gene, respectively.

(D) Wild-type Landsberg *erecta* flower.

(E) Four *ant-9* flowers showing that petals and stamens are narrow and occur in reduced numbers. The right flower is in the C24 background and is more severely abnormal than the other three flowers that are in the Landsberg *erecta* background. Its floral organs are thinner, and the astigmatic carpels are unfused at their apex (arrowhead).

(F) Cleared *ant-9* flower stained with aniline blue and fluoresced to reveal the presence of callose. Pollen tubes, blocked at regular intervals by callose plugs, can be seen in the transmitting tract. The arrowhead shows a band of cells containing callose present in *ant-9* ovules.

(G) and **(H)** *ap2-2* single flower and *ant-9 ap2-2* flowers, respectively. The double mutants lack organs in which sepals, petals, and stamens normally occur, although flowers may be subtended by bractlike organs or filamentous structures. The carpels are often unfused, revealing ovules of the *ant*-conferred phenotype (arrowhead).

(I) Side view of an inflorescence of an *ant-9 ap2-2* double mutant showing the range of flower forms seen and the greatly reduced pedicels (arrowhead).

br, bractlike organ; fs, filamentous structure; pt, pollen tubes. Bars = 2 mm in **(A)** to **(C)** and **(I)**; 1 mm in **(D)**, **(E)**, **(G)**, and **(H)**; and 200 μm in **(F)**.

integuments arise. The mother cell then undergoes meiosis (Figure 2A), with one product undergoing megagametogenesis that results in the mature embryo sac (Figure 2C). In *ant-9* ovules, however, it seems that although the megaspore mother cell arises and generates a tetrad of daughter cells (Figure 2B), megagametogenesis does not occur.

Even so, the mutant nucellus continues to grow and, at maturity, consists of a core of small cells that show moderately heavy staining in sections (Figure 2D). The internal cells lying at the tip where the embryo sac would normally develop are often collapsed and darkly stained. In an occasional *ant-9* ovule, a cell in this region differentiates into a tracheid-like element (data not shown). When mature *ant-9* ovules are stained for the presence of callose, a sector of intensely fluorescent cells occurs in the nucellus-like region. These cells, illustrated in Figure 3F, seem to occupy the central region of this zone and are not distinguishable in toluidine blue–stained sections (Figure 2D).

In mature *ant-9* ovules, a zone of chalaza-like tissue is present adjacent to the nucellus-like cells (Figure 2D). These are large and lightly stained in sections, and the epidermal cells at the nucellar end are particularly large and bulbous. The funiculus of mature *ant-9* ovules is apparently normal.

Ovule abnormalities are most severe in *ant-9* mutants in the genetic background in which the mutant was isolated (C24; Figure 1B). When crossed into the Landsberg *erecta* background, the defects are slightly ameliorated (Figure 1C). Some later growth of large, bulbar epidermal cells now occurs where integuments normally arise, and the mature ovules show a right-angled bend in the region corresponding to the integument–nucellus boundary.

Development of Floral Organs Is Also Affected in *ant-9*

Other parts of the *ant-9* flower are also disrupted. Figure 3 shows their appearance, both in the inflorescence (compare Figures 3B and 3A) and as individual flowers (Figures 3D and 3E). The number of floral organs is often reduced (shown in Table 1), and their shapes may also be modified. Sepals occur in irregular numbers and sizes and are sometimes fused. Their surface is irregular, and the upper edge may be serrated. Petals are narrower and fewer in number than in the wild type (Table 1). In 10% of the flowers, a threadlike organ occurs in place of a petal. Stamens are also reduced in numbers, and the two lateral stamens are usually absent. Both filaments and anthers may be relatively thin, and mosaic organs containing stamen and petal tissue are occasionally seen. The gynoecium is narrow, and its stigmatic papillae are fewer and shorter. It is unfused in 30% of the *ant-9* flowers in the Landsberg *erecta* background, ranging from an unfused stigmatic region to a separation extending down three-quarters of the gynoecial length. Floral organ defects, especially gynoecial defects, are more severe in *ant-9* plants in the original C24 genetic background (Figure 3E).

Conversely, there are very few effects of the *ant-9* mutation on vegetative development. The cotyledons and leaves arise in normal numbers and shapes, and the vasculature of the stem appears normal. Flower numbers are unaffected. Plants are, however, slightly dwarfed and less vigorous than their wild-type siblings.

Floral Organ Development Is Severely Disrupted in *ant-9 ap2-2* Double Mutants

In strong *ap2* mutants, such as *ap2-2*, there are fewer first whorl organs than in the wild type, second whorl organs do not arise, and the number of stamens is greatly reduced (e.g., Figure 3G). *ant-9* mutants also result in a reduction in the number of these organs (Table 1). To test whether *ANT* shares a role with *AP2* in specifying their development, we generated plants mutant for the two loci. Redundant functions would be shown by loss of additional structures and processes still present in each of the single mutants. This proved to be the case, because flowers of the *ant-9 ap2-2* double mutants are markedly different from those of the single mutants (Figures 3H and 3I). The production of all floral organs except carpels is completely abolished. The flowers also lack a pedicel and are usually subtended by a short, thin, threadlike structure or a narrow bract. The gynoecium is relatively unaffected, and the ovules develop essentially as they do in *ant-9* single mutants. However, carpels are unfused to varying degrees in almost all flowers, much more frequently than in either of the single mutants.

Cloning of *ANT* and Complementation of the *ant* Mutant

The locus of the *ant-9* mutant was mapped to the same location as a new *Activator* (*Ac*) insertion (near the bottom of chromosome 4), and the two markers cosegregated among 70 F_2 plants (see Methods). The sequence flanking the 3′ side of the *Ac* insertion was amplified, using inverse polymerase chain reaction (IPCR), and used to identify genomic clones of the region. Figure 4 shows a restriction map of the 17-kb insert of one of these, B19. A region of this clone homologous to the flanking IPCR product was then used to identify cDNA clones from an inflorescence library.

Comparison of the 1.9-kb insert sequence of the largest cDNA (cDNA5) with that of genomic clone B19 revealed that cDNA5 is derived from a 2.65-kb gene composed of eight exons

Table 1. Mean Numbers of Floral Organs in 50 *ant-9* Flowers in the Landsberg *erecta* Background

Floral Organ	Mean No. per Flower (± SE)	Mode	Range
Sepals	3.00 ± 0.11	3	2 to 4
Petals	2.51 ± 0.15	2	0 to 4
Stamens	3.86 ± 0.08	4	2 to 5
Carpels	2.02 ± 0.04	2	1 to 3
Ovules	14.96 ± 0.84	17	10 to 23

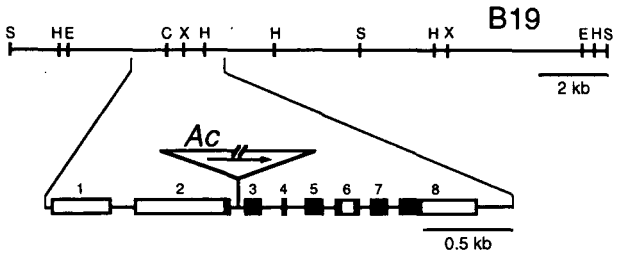

Figure 4. Deduced Structure of the *ANT* Gene and Site of Insertion of the *Ac* Element in the *ant-9* Mutant.

The upper part of the diagram shows a restriction map of genomic clone B19 from wild-type Arabidopsis that contains the *ANT* gene. The map below shows the 5′ and 3′ ends of cDNA5, the eight deduced exons of the *ANT* gene (numbered boxes), the two *AP2* domains within these exons (filled regions of the boxes), and the site of the *Ac* insertion. C, ClaI; E, EcoRI; H, HindIII; S, SalI; X, XhoI.

and seven introns (Figure 4). The gene is interrupted in *ant-9* mutants by an *Ac* element present in intron 2 in the same transcriptional orientation as the disrupted gene (Figure 4). The element is apparently full sized, and PCR sequencing of the border regions showed that 8 bp of intron 2 (nucleotides 1095 to 1102) are duplicated at the insertion site.

We confirmed that this gene corresponds to the *ANT* gene by complementing the *ant-9*–conferred phenotype with a transgenic copy of the wild-type gene (see Methods; Figures 1D and 3C). A 9-kb SalI genomic fragment from B19, including ~3.4 kb upstream of the 5′ end of cDNA5 and 4.0 kb downstream of the poly(A) site (Figure 4), was transformed into wild-type Arabidopsis plants. T_2 plants representing five different primary transformants were then crossed to plants heterozygous for *ant-9*. In F_2 families derived from those that segregated for *ant*, only 4.8% of the plants on average had the *ant*-conferred phenotype. This is close to the expected ratio of 1:16 if *ant-9* is complemented by a segregating transgenic *ANT* gene. However, complementation was not complete. Inspection of the F_2 plants revealed that ~20% of them were the wild type with regard to floral organ development (Figure 3C) but female sterile. These plants were shown to be complemented *ant-9* homozygotes (see Methods). Integument growth of their ovules was partially and variably restored. Some ovules had near normal-sized integuments, whereas in others the nucellus protruded (Figure 1D). Their sterility may have been the consequence of abnormal embryo sac development within the relatively normal ovules. Recently, it has been shown, using other ovule mutants, that embryo sac development is necessary for correct pollen tube guidance to the micropyle in Arabidopsis (Hülskamp et al., 1995) and that pollen tube growth is not directed in this way in the partially complemented plants (results not shown).

Given the similarity in behavior of five independent transgenic lines, it is unlikely that the partial complementation of ovule development results from a position effect of the inserted

```
ATAGAAAGAAGAGAAGCAGAAACCAAAAAAAGAAACCATGAAGTCTTTTTTGTGATAATGA   60
                                M  K  S  P  C  D  N  D     8

TGATAATAATCATAGCAACACGACTAATTTGTTAGGGTTCTCATTGTCTTCAAATATGAT  120
 D  N  N  H  S  N  T  T  N  L  L  G  F  S  L  S  S  N  M  M    28

GAAAATGGGAGGTAGAGGAGGTAGAGAAGCTATTTACTCATCTTCAACTTCTTCAGCTGC  180
 K  M  G  G  R  G  G  R  E  A  I  Y  S  S  S  T  S  S  A  A    48

AACTTCTTCTTCTTCTGTTCCACCTCAACTTGTTGTTGGTGACAACACTAGCAACTTTGG  240
 T  S  S  S  S  V  P  P  Q  L  V  V  G  D  N  T  S  N  F  G    68

TGTTTGCTATGGATCTAACCCAAATGGAGGAATCTATTCTCACATGTCTGTGATGCCACT  300
 V  C  Y  G  S  N  P  N  G  G  I  Y  S  H  M  S  V  M  P  L    88

CAGATCTGATGGTTCTCTTTGCTTAATGGAAGCTCTCAACAGATCTTCTCACTCGAATCA  360
 R  S  D  G  S  L  C  L  M  E  A  L  N  R  S  S  H  S  N  H   108

CCATCAAGATTCATCTCCAAAGGTGGAGGATTTCTTTGGGACCCATCACAACAACACAAG  420
 H  Q  D  S  S  P  K  V  E  D  F  F  G  T  H  H  N  N  T  S   128

TCACAAAGAAGCCATGGATCTTAGCTTAGATAGTTTATTCTACAACACCACTCATGAGCC  480
 H  K  E  A  M  D  L  S  L  D  S  L  F  Y  N  T  T  H  E  P   148

CAACACGACTACAAACTTTCAAGAGTTCTTTAGCTTCCCTCAAACCAGAAACCATGAGGA  540
 N  T  T  T  N  F  Q  E  F  F  S  F  P  Q  T  R  N  H  E  E   166

AGAAACTAGAAATTACGGGAATGACCCTAGTTTGACACATGGAGGGTCTTTTAATGTAGG  600
 E  T  R  N  Y  G  N  D  P  S  L  T  H  G  G  S  F  N  V  G   188

GGTATATGGGGAATTTCAACAGTCACTGAGCTTATCCATGAGCCCTGGGTCACAATCTAG  660
 V  Y  G  E  F  Q  Q  S  L  S  L  S  M  S  P  G  S  Q  S  S   208

CTGCATCACTGGCTCTCACCACCACCAACAAAACCAAAACCAAAACCACCAAAGCCAAAA  720
 C  I  T  G  S  H  H  H  Q  Q  N  Q  N  Q  N  H  Q  S  Q  N   228

CCACCAGCAGATCTCTGAAGCTCTTGTGGAGACAAGCGTTGGGTTTGAGACGACGACAAT  780
 H  Q  Q  I  S  E  A  L  V  E  T  S  V  G  F  E  T  T  T  M   248

GGCGGCTGCGAAGAAGAAGAGGGGACAAGAGGATGTTGTAGTTGTTGGTCAGAAACAGAT  840
 A  A  A  K  K  K  R  G  Q  E  D  V  V  V  V  G  Q  K  Q  I   268

TGTTCATAGAAAATCTATCGATACTTTTGGACAACGAACTTCTCAATACCGAGGCGTTAC  900
 V  H  R  K  S  I  D  T  F  G  Q  R  T  S  Q  Y  R  G  V  T   288

AAGACATAGATGGACTGGTAGATATGAAGCTCATCTATGGGACAATAGTTTCAAGAAGGA  960
 R  H  R  W  T  G  R  Y  E  A  H  L  W  D  N  S  F  K  K  E   308

AGGTCACAGTAGAAAAGGAAGACAAGTTTATCTGGGAGGTTATGATATGGAGGAGAAAGC 1020
 G  H  S  R  K  G  R  Q  V  Y  L  G  G  Y  D  M  E  E  K  A   328

TGCTCGAGCATATGATCTTGCTGCACTCAAGTACTGGGGTCCCTCTACTCACACCAATTT 1080
 A  R  A  Y  D  L  A  A  L  K  Y  W  G  P  S  T  H  T  N  F   348

CTCTGCGGAGAATTATCAGAAAGAGATTGAAGACATGAAGAACATGACTAGACAAGAATA 1140
 S  A  E  N  Y  Q  K  E  I  E  D  M  K  N  M  T  R  Q  E  Y   368

TGTTGCACATTTGAGAAGGAAGAGCAGTGGTTTCTCTAGGGGTGCTTCCATCTATAGAGG 1200
 V  A  H  L  R  R  K  S  S  G  F  S  R  G  A  S  I  Y  R  G   388

AGTCACAAGACATCACCAGCATGGAAGGTGGCAAGCACGGATTGGTAGAGTCGCTGGAAA 1260
 V  T  R  H  H  Q  H  G  R  W  Q  A  R  I  G  R  V  A  G  N   408

CAAAGATCTCTACCTTGGAACTTTTGGAACCCAAGAAGAAGCTGCAGAAGCTTACGATGT 1320
 K  D  L  Y  L  G  T  F  G  T  Q  E  E  A  A  E  A  Y  D  V   428

AGCAGCAATTAAGTTCCGTGGCACAAATGCTGTGACTAACTTTGATATCACGAGGTACGA 1380
 A  A  I  K  F  R  G  T  N  A  V  T  N  F  D  I  T  R  Y  D   448

TGTTGATCGTATCATGTCTAGTAACACACTCTTGTCTGGAGAGTTAGCGCGAAGGAACAA 1440
 V  D  R  I  M  S  S  N  T  L  L  S  G  E  L  A  R  R  N  N   468

CAACAGCATTGTCGTCAGGAATACTGAAGACCAAACCGCTCTAAATGCTGTTGTGGAAGG 1500
 N  S  I  V  V  R  N  T  E  D  Q  T  A  L  N  A  V  V  E  G   488

TGGTTCCAACAAAGAAGTCAGTACTCCCGAGAGACTCTTGAGTTTTCCGGCGATTTTCGC 1560
 G  S  N  K  E  V  S  T  P  E  R  L  L  S  F  P  A  I  F  A   508

GTTGCCTCAAGTTAATCAAAAGATGTTCGGATCAAATATGGGCGGAAATATGAGTCCTTG 1620
 L  P  Q  V  N  Q  K  M  F  G  S  N  M  G  G  N  M  S  P  W   528

GACATCAAACCCTAATGCTGAGCTTAAGACCGTCGCTCTTACTTTGCCT AGATGCCGGT 1680
 T  S  N  P  N  A  E  L  K  T  V  A  L  T  L  P  Q  M  P  V   548

TTTCGCTGCTTGGGCTGATTCTTGATCAACTTCAATGACTAACTCTGGTTTTCTTGGTTT 1740
 F  A  A  W  A  D  S  *

AGTTGCTAAGTGTTTTGGTTTATCTCCGGTTTTATCCGGTTTGAACTACAATTCGGTTTA 1800

GTTTCGTCGGTATAAATAGTATTTGCTTAGGAGCGGTATATGTTTCTTTTGAGTAGTATT 1860

CATGTGAAACAGAATGAATCTCTCTATAACATATTATTTTAATGGAAAAAAAAAAAAAAA 1920
```

Figure 5. Full Sequence of *ANT* cDNA5 and Deduced Sequence of the ANT Protein.

The locations of the seven introns are indicated with inverted triangles. The two tandemly repeated AP2 domains are underlined with double lines, and the putative serine-rich and glutamine-rich activation domains are underlined with single lines.

```
ANT R1                                [SFKKEGHSRK]
ZM R1                                 [*CRR**Q***]

ANT R1  TSQYRGVTRH RWTGRYEAHL WDN|-GRQVY LGGYDMEEKA ARAYDLAALK YWGPSTHTNF SAENYQKEI
ZM  R1  **I******* ********** *N*|-***** *****K**** ********** F***T*T*** QVS**E**L
AP2 R1  S*******FY *R***W*S*I **C--*K*** ***F*TAHA* *****R**I* FR*VEADI** NIDD*DDDL

ANT R2  ASIYRGVTRH HQHGRWQARI GRVAGNKDLY LGTFGTQEEA AEAYDVAAIK FRGTNAVTNF DITRYDVDR
ZM  R2  ********** ********** *S******** ****S***** *****I**** ***L****** *MS****ES
AP2 R2  S*K*****L* KC-***E**M *QFL*K*YV* **L*D*EV** *R***K**** CN*KD***** *PSI**EEL

          s YRGVt      gr              y LG _____ A A AYD AA k__ G     NF     y

EREBP-1 GRHYRGVRRR PWGKFAAEIR DPAKNGARVW LGTYETDEEA AIAYDKAAYR MRGSKAHLNF PHRIGLNEP
```

Figure 6. Alignment of the AP2 Domains of *ANT* with Those of Three Related Genes.

Shown is the the first repeat (R1) for *ANT*, its putative ortholog from maize (ZMMHCF1 [ZM]), and the *AP2* R1 domain (Jofuku et al., 1994). Both *ANT* and the maize sequence contain an insertion of 10 amino acids after codon 23. The alignment of the second repeat (R2) for the same three genes is also shown. Amino acids shared with ANT are shown with asterisks in each case. Gaps are indicated by dashes. The single repeat present in a tobacco ethylene response element binding protein (EREBP-1; Ohme-Takagi and Shinshi, 1995) is also presented. The consensus sequence is indicated with uppercase letters for amino acids shared by all seven domains and as lowercase letters for those found in the six duplicated domains but not in the single EREBP-1 domain. The region predicted to generate an amphipathic α-helix is underlined (Jofuku et al., 1994).

transgene. Also, similarities in the phenotype of *ant-9* and other *ant* mutants (Reiser and Fischer, 1993) mean that it is unlikely that an uncomplemented mutation is present at a second site in *ant-9*. Rather, the activity of the transgene may be insufficient to restore ovule development fully, although sufficient to allow wild-type floral organs to arise.

The *ANT* Gene Encodes a Putative Transcription Factor Containing Two AP2 Domains

Figure 5 shows that cDNA5 contains an insert of 1905 nucleotides. An open reading frame of 555 codons occurs within this insert. It begins at the first methionine 38 bp from the 5′ end and ends 199 bp before the poly(A) tail. Translation of the cDNA sequence showed that *ANT* encodes a putative protein related to the *AP2* gene product of Arabidopsis (Jofuku et al., 1994). The AP2 protein contains two tandemly repeated 68–amino acid motifs designated AP2 domains (Jofuku et al., 1994). These are also found in *ANT*, and Figure 6 shows that each domain has >50% amino acid sequence identity with those in the AP2 protein. Significantly, the region between the two domains is also conserved between ANT and AP2, with 13 of the 25 linking residues being identical (data not shown). Otherwise, the two proteins show little recognizable similarity.

Recently, four proteins that bind to specific DNA sequences found in ethylene response elements of tobacco have been described (Ohme-Takagi and Shinshi, 1995), and their DNA binding domain was shown to be related to the AP2 domain (Weigel, 1995; Figure 6). Because *ANT* and *AP2* both share this conserved domain, it seems that they too are transcription factor genes. ANT contains a serine-rich sequence of 13 amino acids near its N terminus and a glutamine/asparagine/histidine–rich sequence extending from codon 214 to 231 (Figure 5). Such serine- and glutamine-rich sequences are characteristic of transcriptional activation domains by which transcription factors interact with basal proteins of the transcriptional apparatus (Mitchell and Tjian, 1989).

It is clear that the AP2 domain is present in a large family of plant genes (Jofuku et al., 1994; Weigel, 1995), although most have only one AP2 domain, and many have been identified only as expressed sequence tags of unknown function. Sequence comparisons showed that ANT is most closely related to members that contain two repeats, including AP2 of Arabidopsis and the ZMMHCF1 sequence of maize. The latter is the likely ortholog of ANT and is a cDNA sequence derived from postpollination maize endosperm (GenBank accession number Z47554; unpublished data of T.J. Daniell and R. Edwards, Durham University, Durham, UK). It contains two tandemly repeated AP2 domains that are 84% identical to the ANT repeats. This identity is much greater than the 56% shown between ANT and AP2 (Figure 6). Furthermore, the first repeat contains a 10–amino acid insertion that is also found in ANT but not in AP2 or in single AP2 domain proteins. Intron splicing sequences are found in the nucleic acid sequences corresponding to the beginning and end of this insert, indicating that the insert may have arisen from the expression of a former intron. Even though the *AP2* domains and the link between them are highly conserved between ANT and the maize ortholog, the two putative proteins show little sequence similarity elsewhere.

ANT Is Expressed in Developing Ovules and in the Primordia of Other Floral and Vegetative Organs

ANT expression was examined by in situ hybridization of a ^{35}S-labeled antisense probe with tissue sections of inflores-

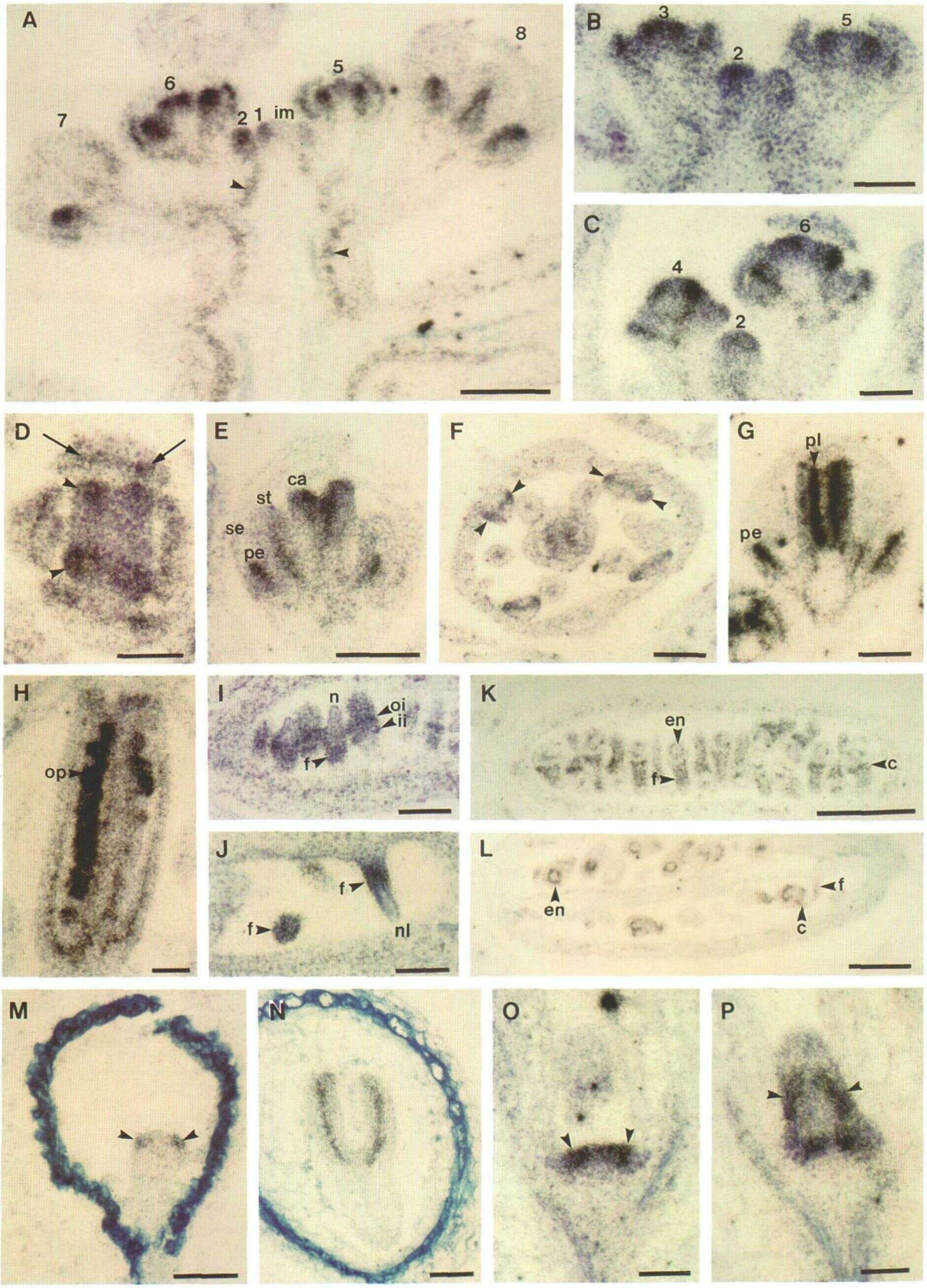

Figure 7. In Situ Hybridization of ^{35}S-Labeled Antisense cDNA of *ANT* with Floral and Vegetative Organs.

cences, flowers, developing seed, and seedlings. The results are illustrated in Figure 7. In general, *ANT* is expressed not only in developing ovules but also in the primordia of all other floral organs, cotyledons, and leaves. Results for flower organs, where patterns are particularly complex, are summarized in Figure 8.

In the inflorescence, *ANT* expression is either low or absent in the apical meristem itself, although it is expressed in procambial cells of the developing stem (Figure 7A). The first heavy labeling occurs in the newly arising flower primordia (stage 1; Smyth et al., 1990). As these separate from the flank of the inflorescence meristem (stage 2; Figures 7A and 7B), *ANT* expression is gradually localized to regions that will give rise to sepal primordia. The expression in sepals continues from when they arise at stage 3 (Figure 7B) to about the time they fully enclose the bud (stage 6; Figures 7C and 7D). Initially, all sepal cells are labeled, but expression is gradually reduced to a core at the sepal's base before finally disappearing.

ANT expression appears in regions that will give rise to stamens in stage 3 buds (Figure 7B), well before they arise at stage 5. Expression occurs initially in all cells of stamen primordia (Figure 7C) but is confined to a central region as they become stalked (stage 7; Figure 7E) and develop locules (stage

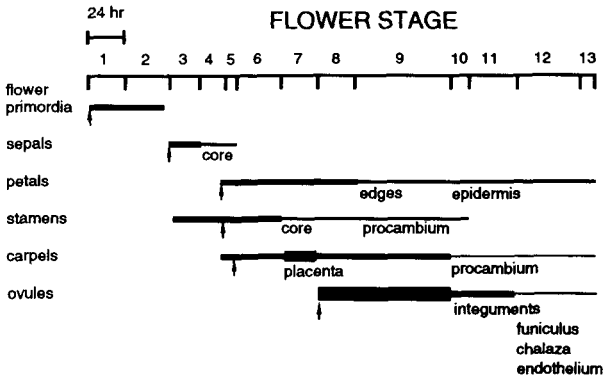

Figure 8. Summary of *ANT* Expression Patterns in Developing Flowers as Deduced from in Situ Hybridization Experiments.

The stages and their durations are from Smyth et al. (1990). The relative thickness of lines reflects the level of labeling observed (see Figure 7). Arrows define the times at which primordia arise. For all types of primordia, labeling occurs throughout as they arise. As the labeling becomes localized, its specific site(s) within each organ is indicated.

Figure 7. (continued).

All sections are from wild-type Landsberg *erecta*, except for the section shown in **(J)**, which is *ant-9*. Numbers refer to the stage of flower development reached by individual buds (Smyth et al., 1990).

(A) Longitudinal section of an inflorescence apex showing strong labeling in flower and floral organ primordia, some labeling in procambium cells (arrowheads), but no label detectable in the apex of the inflorescence meristem.

(B) Higher magnification of an inflorescence apex with early-stage buds.

(C) More advanced buds showing that regionalization of label is occurring within flower and floral organ primordia.

(D) Transverse section toward the top of a stage 6 bud showing labeling concentrated in the primordia of the medial stamens (arrowheads) and in internal zones of the four sepals (arrows).

(E) Oblique longitudinal section of a stage 7 bud showing labeling of petal primordia, the core of developing stamens, and the top and inside of the growing gynoecium.

(F) Transverse section of a stage 9 bud in which label is heaviest in the two lateral edges of the growing petals (arrowheads).

(G) Longitudinal section of a stage 8 bud in which the placenta is heavily labeled, as are other regions of the gynoecium and the elongating petals.

(H) Longitudinal section of a stage 9 gynoecium in which the ovule primordia are intensely and uniformly labeled.

(I) Longitudinal section of wild-type ovules in which the integuments are arising (stage 11), showing that labeling is present in the two bands of integument cells and in the adjoining distal region of the funiculus. The nucellus and the base of the funiculus show little if any labeling.

(J) Longitudinal section of *ant-9* ovules showing reduced but significant labeling in the region of the funiculus close to where integuments would normally have arisen (arrowheads).

(K) Longitudinal section of a gynoecium in the medial plane from a stage 12 flower showing that the developing ovules are labeled in the funiculus, in the chalaza at the base of the ovule proper, and in the newly arising endothelium derived from the inner integument.

(L) Longitudinal section of a gynoecium in the lateral plane from a mature stage 13 flower in which labeling continues in the funiculus, the chalaza, and the cup-shaped endothelium.

(M) Section of a developing seed showing two zones of significant labeling in the globular-stage embryo, where cotyledons are likely to arise (arrowheads).

(N) Section of a seed at a later stage in which the cotyledons of the torpedo-stage embryo are labeled internally.

(O) and **(P)** Longitudinal sections of a seedling at the two-leaf stage showing zones of labeling on the flanks of the apical meristem where new leaves may arise (arrowheads in **[O]**) and bands of internal labeling in a newly arisen leaf (arrowheads in **[P]**). **(O)** and **(P)** are from a group of serial sections and are separated by two 8-μm sections.

c, chalaza; ca, carpel; en, endothelium; f, funiculus; ii, inner integument; im, inflorescence meristem; n, nucellus; nl, nucellus-like structure; oi, outer integument; op, ovule primordium; pe, petal; pl, placenta; se, sepal; st, stamen. Bars = 100 μm in **(A)** and **(E)** to **(G)**; 50 μm in **(B)** to **(D)**, **(H)** to **(J)**, **(M)**, and **(N)**; and 200 μm in **(K)**, **(L)**, **(O)**, and **(P)**.

8; Figure 7G). Ultimately, expression is reduced to procambial cells, especially in the filaments, as the stamens mature.

Petal primordia appear between the developing sepals at the same time as stamen primordia (stage 5; Figure 7B). Initially, they are very small, but strong *ANT* expression is clearly apparent from their earliest appearance (Figures 7C and 7E). As petal primordia become peltate (stage 9), expression is stronger along their lateral edges, which are rapidly extending (Figure 7F). Lower but significant expression continues as the petals elongate during stages 11 and 12, by which time labeling is mostly localized to the epidermis. Expression could not be detected in mature petals as the bud opens (stage 13).

In the carpels, *ANT* expression appears in the apical part of the flower primordium at stage 5 (Figure 7A). Once carpel primordia arise from this region and elongate to generate a hollow cylinder (from stage 6; Figure 7C), expression increases on the inner surface (Figure 7E) and reaches very high levels in the placenta (Figure 7G). Low *ANT* expression also occurs in the developing carpel walls but not in stigmatic papillae or septal tissues. Procambial cells in the gynoecium are also labeled (Figure 7H).

Very strong levels of *ANT* expression are maintained in ovule primordia from the time they arise from the placenta during stage 8 (Figure 7G) and elongate during stage 9 (Figure 7H). However, expression does not occur in the nucellus that develops at the apex of the ovule primordium at around this time (stage 10; Figure 7I). Instead, it becomes focused in regions in which the inner and outer integuments will arise in quick succession (Figure 7I). The integuments are specifically labeled through their early growth phase, but labeling decreases in the outer integument as it covers the nucellus during stage 11. It becomes localized in inner integument cells that will differentiate into the endothelium during stage 12 (Figure 7K) and is maintained there until stage 13 (Figure 7L). *ANT* expression occurs in the distal half of the funiculus throughout ovule development (Figures 7I, 7K, and 7L) and extends into a broader region at the base of the ovule proper (the chalaza; Figures 7K and 7L).

After fertilization, *ANT* expression shifts to the embryo. There appear to be two regions of expression in globular-stage embryos, presumably in cells that will give rise to the cotyledons (Figure 7M). Later, at the torpedo stage, *ANT* is expressed in cells in an internal zone extending the length of each cotyledon (Figure 7N). These may include procambial cells that will ultimately give rise to the vasculature. The embryonic hypocotyl and root show no labeling. When *ANT* expression was examined in young seedlings at the two-leaf stage, the shoot apical meristem contained discrete zones of labeling in its periphery, presumably indicating where leaf primordia would ultimately arise (Figure 7O). Also, developing leaves contained two internal zones of expression extending longitudinally down each side (Figure 7P), very similar to that seen in developing sepals (Figure 7D). Root meristems showed no evidence of *ANT* expression, and neither did mature tissues of roots, stems, and leaves.

The transcription of *ANT* is reduced but not eliminated in *ant-9* plants. Preliminary RNA gel blot results showed that a transcript of wild-type length is not produced but that there are two new transcripts presumably associated with premature termination and missplicing within the *Ac* insert. Thus, *ant-9* is likely to be a null mutation. The tissue-specific patterns of expression in *ant-9* mutants did not diverge markedly from that of the wild type, suggesting that autoregulation of *ANT* expression does not occur. In regions of *ant-9* ovule primordia where integuments would normally develop, significant expression could be detected (Figure 7J). Even though subsequent ovule development is abnormal, expression is maintained in this region and in much of the funiculus until at least stage 13.

In summary, *ANT* expression is particularly strong in ovule primordia and is associated with integuments that arise from these primordia. However, expression also occurs in the primordia of all other organ types of the developing plant, with the sole exception of roots.

DISCUSSION

The *ANT* gene appears to have two major roles in development. First, it plays a major part in the morphogenesis of ovules. Second, it is likely to have a general role in the initiation and growth of vegetative and floral organ primordia. The first role is clearly revealed by the abnormal ovule phenotype in *ant* mutants, whereas the second role is inferred from the loss of organs in *ant-9* plants and the expression pattern of *ANT* in wild-type primordia.

Role of *ANT* in Ovule Development

The first defect seen in *ant-9* mutant ovules is that no integuments arise. Expression of *ANT* occurs in wild-type cells that will generate the integuments, and it is maintained within them during their early growth. Thus, ANT presumably has a direct role in controlling integument initiation and growth.

sup mutants also exhibit specific defects in integument development, although their growth is promoted rather than abolished (Gaiser et al., 1995). Thus, the wild-type SUP product may limit the extent of integument proliferation (Sakai et al., 1995). Because *SUP* is not expressed in the integuments but rather in the funiculus, this action is presumably nonautonomous (Sakai et al., 1995). If SUP integument function were negatively controlled by the ANT product, SUP would show increased function in *ant* mutants, thereby accounting for the complete suppression of integument growth. This proposal can be tested by examining the levels of SUP expression and activity in *ant* ovules.

The second consequence of the loss of ANT function seen in ovules is the absence of the megaspore and embryo sac. This is unexpected given that *ANT* is not expressed in the

nucellus, where the megaspore arises. Several hypotheses can be proposed to account for this. First, the mutant effect may be a delayed consequence of the loss of earlier ANT function in nucellus precursor cells. Alternatively, ANT could be acting in a non–cell autonomous fashion. It is possible that *ANT* expression in the newly arising integuments is involved in setting up a morphogenetic gradient in the nucellus and that this gradient determines that the meiotic product closest to the integuments does not degenerate. When *ANT* activity is absent or reduced, all products abort.

The late expression of *ANT* in the chalaza and endothelium of the maturing ovule could not have been predicted from the *ant*-conferred phenotype. Because mutant disruption occurs much earlier in ovule development, the endothelium does not arise, and growth in the chalazal region is much reduced. The role of *ANT* in these tissues is not clear, although its late expression in the endothelium is shared with the floral homeotic gene *AG* (Bowman et al., 1991a). Also, it is interesting that the expression of *ANT* in the funiculus is not mirrored by defects in funicular structure in *ant-9* mutants, and ANT function in the funiculus may be performed redundantly by other genes that can mask its loss.

Finally, two aberrant differentiation events occur late in *ant-9* ovule development. First, a band of callose appears in the nucellus-like outgrowth. Callose is generally found surrounding the four megaspores in wild-type ovules (Schneitz et al., 1995) and later in cells at the base of the embryo sac and/or the endothelium (Kapil and Tiwari, 1978). It may be that the abnormal cells in the *ant* mutant reflect the ectopic execution of the developmental program of the latter cells. Second, the occasional development of a tracheid at the tip of the *ant-9* ovule is a phenomenon also reported in *bel* mutants (Ray et al., 1994; Herr, 1995). This may reflect the aberrant *trans*-determination of a developmental program well downstream of the primary site of mutant disruption. Alternatively, it has been proposed that this observation supports a possible evolutionary link between vasculature and sporogenous tissues (Herr, 1995).

General Role of *ANT* in Promoting Primordium Initiation and Growth

The expression pattern of *ANT* is consistent with it having a general role in primordium initiation. All organ primordia except roots are involved. Expression also occurs in the newly arising vasculature, the procambium. *ANT* expression appears very early in organ development, in some cases before the primordia arise, as expected for a gene controlling organ initiation. When ANT function is lost in *ant-9* mutants, ovule primordia and all four classes of floral organs arise in fewer numbers, although the loss is almost never complete. There are no homeotic transformations, and mature structures are relatively normal. This suggests that the primary role of ANT is to contribute to organ initiation without being absolutely required for any organ type. On the other hand, other primordial cells that also express ANT display no mutational disruption. These include cotyledons, leaves, and the procambium in stems. ANT could control the initiation of these unaffected organs and tissues as well, but the function may be redundantly shared with other genes.

Once organs have been initiated, their early growth may also be influenced by ANT function. After its initial expression throughout the primordia, *ANT* expression soon becomes confined to specific areas, especially those where active growth is occurring. In some cases, these growing zones correspond to regions defective in mutant organs. For example, petals in *ant* mutants are usually very narrow, consistent with relatively late expression of *ANT* at their margins. Growth defects can also account for the ragged edges of sepals, the thin stamens, and the narrow, unfused carpels regularly seen in *ant-9* flowers.

ANT and *AP2* Functions Overlap

The striking synergistic phenotype of the *ap2 ant* double mutant reveals that some functions of *ANT* overlap with those of *AP2*. One function of *AP2* is the cadastral repression of *AG* in the first two whorls of the flower (Drews et al., 1991). When this function is lost, ectopic *AG* expression apparently results in the reduction or loss of these organs through the growth-suppression effects of *AG* (Bowman et al., 1991b). *ANT* may have a similar role in blocking *AG* expression. Evidence for this comes from the *ant-9 ap2-2* double mutant phenotype. Some organs develop in each single mutant, but all are abolished in the double. That is, the full effect of AG on suppressing the initiation of organs in this region requires the loss of both AP2 and ANT activity. This predicts that *AG* expression occurs ectopically in the outer whorls of *ant-9* flowers, as seen in *ap2* mutants (Drews et al., 1991). Tests of such ectopic expression are now under way.

However, in addition to its role in suppressing growth, *AG* has a role in specifying floral organ identity (Bowman et al., 1989, 1991b). It seems that this latter function is not ectopically expressed in *ant* mutants because the identity of the first and second whorls is not affected. It may be that when ANT function is lost by mutation, the remaining AP2 function is fully effective in preventing *AG* expression in the first two whorls. That is, the cadastral aspect of ANT function is fully encompassed by that of AP2. Alternatively, ANT may not have a cadastral role at all, and the effect of ANT on *AG* occurs only when ectopic expression of the latter is allowed in the first two whorls, for example, when AP2 function is lost. In this case, the *ANT* gene product would be able to antagonize some of the growth-suppression effects of AG but not the organ-identity effects.

Recently, another gene, *LEUNIG* (*LUG*), has been shown to share a role with *AP2* in inhibiting *AG* function in the first two whorls. Double mutants of *lug* and *ap2* are very similar in phenotype to *ant ap2* double mutants in that all outer floral

organs are lost, and the flower appears as a solitary gynoecium usually subtended by a bract (Liu and Meyerowitz, 1995). However, unlike *ant*, *lug* single mutants reveal organ-identity changes in the first two whorls (Liu and Meyerowitz, 1995). Thus, *LUG*, like *AP2*, may have a more direct effect on preventing *AG* expression in the outer whorls than does *ANT*. In this case, the similar effects of *ant* and *lug* mutations when in an *ap2* mutant background would have different origins: for LUG, they would be the consequence of the loss of its cadastral role; for ANT, the loss of its role in the initiation of primordia would be the cause. If the latter is correct, the stronger phenotype of *ant ap2* double mutants has uncovered and highlighted a direct role for AP2 in primordium initiation (Bowman et al., 1991b).

AG has also been shown to have effects in ovule development. In strong *bel* mutants, integuments are often homeotically transformed into carpel/sepal–like organs (Modrusan et al., 1994; Ray et al., 1994). This transformation is associated with ectopic *AG* expression in the developing integuments and is also seen in plants containing a constitutively expressed *AG* transgene (Ray et al., 1994). For *AG*, it has been reported recently that suppression of growth requires higher levels of AG activity than does the specification of organ identity (Mizukami and Ma, 1995; Sieburth et al., 1995). If very high levels of AG activity were present in *ant* mutant ovules as a consequence of the loss of ANT activity in cadastrally preventing *AG* expression, this could result in the observed suppression of integument growth rather than their homeotic conversion.

ANT Redundancy and Interaction with Other Genes

As a putative transcription factor, the *ANT* gene product is likely to interact with a range of other transcription factors and coactivators of the transcription process. These interactions might often occur in a redundant way, with other transcription factors being capable of substituting for some or all of the ANT interactions and vice versa. Functional redundancy could also arise if different transcription factors shared target genes whose expression could be regulated by either transcription factor.

It is probable that *ANT* interacts with some members of its own transcription factor family. We have already suggested that *ANT* and *AP2* redundantly share functions in promoting floral organ growth. The more distantly related AP2 domain family members, such as those encoding ethylene response element binding proteins, probably have functions unrelated to *ANT*. In this regard, ethylene appears to play little role in flower morphogenesis, with the exception of a reported post-pollination triggering of ovule development in orchids (Zhang and O'Neill, 1993). The AP2 domain family has two groups: in one the proteins have only one AP2 domain; in the other, they have two in tandem (Weigel, 1995). A duplication event generating the tandem copies within the protein apparently occurred relatively early in plant evolution, at least before the monocot–dicot divergence. This is because the Arabidopsis *ANT* gene has a maize ortholog of closely similar sequence. Presumably, the subsequent duplication of the two-domain gene to generate the ancestors of *ANT* and *AP2* also occurred sufficiently long ago to allow for evolutionary divergence in their sequence and function.

There are many other candidate transcription factor genes whose actions may be redundant with that of *ANT*. For example, a range of *AG*-like genes is known whose expression patterns indicate that they could serve as *ANT* partners (Angenent et al., 1995; Rounsley et al., 1995). None of the patterns matches exactly that of *ANT*, but many overlaps occur. Another large transcription factor family is characterized by the possession of a *Knotted1*-like (*Kn1*-like) homeodomain. In maize, *Kn1* and certain related genes are expressed in developing shoot apical meristems (Jackson et al., 1994). In many ways, the expression pattern of *Kn1*-like genes is complementary to that of *ANT*, and interactions with ANT in this case may take the form of mutual antagonism.

The challenge now is to identify other transcription factors with which *ANT* interacts physically, the genes they control, and the mechanisms by which these events combine to generate the detailed form of the higher plant body.

METHODS

Isolation and Mapping of the *aintegumenta-9* Mutant

To obtain *Activator* (*Ac*)-tagged mutants, the binary vector p35SAc12 was used (Finnegan et al., 1993). This vector contains the maize *Ac* element under the control of the cauliflower mosaic virus 35S promoter and was transformed into *Arabidopsis thaliana* ecotype C24, using the *Agrobacterium tumefaciens* root transformation protocol of Valvekens et al. (1988). Female-sterile mutant 243-1 was identified among descendants of one transformant and rescued by outcrossing to a Columbia line. It was then crossed to a Landsberg *erecta* line and made homozygous for the *erecta* mutation. In subsequent generations, the mutation segregated as a single recessive allele that was given the preliminary name *wormy ovules-1*. Preliminary data showed that a new *Ac* insertion was strictly present in 20 homozygous mutant F_2 plants and in 50 heterozygotes.

To map the site of the new *Ac* insert, a cloned border fragment (p3015; see below) was used. This revealed an EcoRI polymorphism between Landsberg *erecta* and Niederzenz ecotypes that mapped to the bottom of chromosome 4, approximately five map units (two recombinants of 36 chromosomes) below the restriction fragment length polymorphism marker m214. The locus of the mutant was also mapped to this region. When crossed with the *spatula-2* mutant, F_2 segregation data revealed that its locus lies approximately two to three map units below the *SPATULA* locus (M. Heisler, personal communication), which in turn lies just below *APETALA2* (*AP2*).

Toward the end of this study, it became apparent that the phenotype of our female-sterile mutant was similar to that of ovule mutants isolated by others. Allelism with a mutant originally named *ovule mutant3* (Reiser and Fischer, 1993) was established by exchanging a limited region of amino acid sequence with R. Fischer at the University of California, Berkeley. To test allelism with another mutant initially called

dragon, C. Gasser (University of California, Davis) kindly provided seed of *dragon-4*. After crossing our mutant with *dragon-4* heterozygotes, we obtained F_1 progeny in which approximately half of the plants showed the mutant phenotype, thus proving allelism with this line as well. By agreement, the gene has been named *AINTEGUMENTA* (*ANT*), and our mutant allele has been designated *ant-9*.

Generation of *ant-9 ap2-2* Double Mutants

To obtain double mutants of *ant-9* and the strong mutant allele *ap2-2* (Bowman et al., 1991b), the two lines (both in the Landsberg *erecta* background) were crossed, and a series of 100 F_2 plants with the *ap2*-conferred phenotype was allowed to self-fertilize. Among the resulting F_3 families, two contained plants with a new, more severely disrupted phenotype. One of these plants was shown by polymerase chain reaction (PCR) to be homozygous for *ant-9* and therefore an *ant-9 ap2-2* double mutant. Tests using appropriate primers revealed that it carried the *Ac* insert within *ANT* but lacked the uninterrupted form of the gene. The two F_3 families were apparently derived from F_2 parents that carried a chromosome that had recombined between the closely linked *ANT* and *AP2* loci.

Cloning of the *ANT* Gene and *ANT* cDNA

The region 3′ to the new *Ac* insert was cloned by inverse PCR (IPCR; Ochman et al., 1990). DNA from *ant-9* plants was digested with HindIII, religated, cut with XbaI, and amplified with primers from the 3′ end of *Ac* (5′-AGATGCTGCTACCCAATCTTTTGTGCA-3′, and 5′-CGTATCGGTTTTCGATTACCGTATTT-3′). The IPCR product was cloned into the SmaI site of pBluescript SK+ (Stratagene) and named p3015.

p3015 was used to screen a phage λ EMBL4 genomic library of Landsberg *erecta* DNA. Three positive clones were isolated, and one (B19) was selected for further analysis (Figure 4). Portions of λ B19 surrounding the p3015-homologous sequences were used to screen a cDNA library made from Arabidopsis inflorescence RNA (ecotype Landsberg *erecta*) in phage λ ZAP II (Stratagene), kindly provided by D. Weigel (Salk Institute, La Jolla, CA). Two cDNA clones that cross-hybridized with p3015 and with each other were isolated. The longer clone, cDNA5, was used as a probe to rescreen the library, isolating an additional five cDNA clones. The longest of these was ~1.9 kb, which is the same length as cDNA5. To screen for longer transcripts, reverse transcriptase PCR was applied to an inflorescence RNA preparation, using forward primers at −410, −237, and +159 relative to the 5′ end of cDNA5 and a reverse primer downstream of the first intron. Of the forward primers, only the +159 primer amplified a product successfully. This, together with the absence of significant open reading frames in the region −410 to +1, suggests that cDNA5 encodes the complete ANT protein.

Both strands of the cDNA5 insert and a total of 4 kb of the genomic clone B19 were sequenced using DyeDeoxy termination cycle sequencing (Perkin-Elmer, Applied Biosystems Division, Foster City, CA), and the cDNA sequence has the GenBank accession number U41339. Sequence comparisons were performed at the National Center for Biotechnology Information, using the BLAST network service.

Complementation of *ant-9*

A 9-kb SalI fragment surrounding the genomic *ANT* sequence in B19 (Figure 4) was subcloned into the binary vector pBIN19 and then transformed into Landsberg *erecta* roots, using the protocol of Valvekens et al. (1988). Five different transformants in which kanamycin resistance segregated as expected for a single active insert were obtained. These transformants were then crossed as T_2 plants to *ant-9* heterozygotes, and F_2 progeny were raised for each. The *ANT* genotype of individual plants that were putatively complemented was confirmed by using a probe derived from a part of the genomic clone B19 downstream of the *ANT* gene. This probe does not hybridize with the transgenic version of *ANT* but allows the endogenous *ant-9* and *ANT* alleles to be distinguished through a polymorphic HindIII site that is present in the *ant-9* strain C24 but absent in the cosegregating wild-type Landsberg *erecta* allele.

Microscopy and in Situ Hybridization

Scanning electron microscopy was performed as described by Bowman et al. (1993). For tissue sections, buds were fixed for 18 hr in 2% glutaraldehyde in 0.025 M phosphate buffer, pH 6.8, rinsed, dehydrated through an ethanol series, and embedded in LR White (London Resin Co. Ltd., Basingstoke, England). Sections of 2 μm were cut and stained with 0.1% toluidine blue, pH 9.0. Fluorescent staining of callose with aniline blue was performed on flowers fixed for 30 min in 3:1 (v/v) ethanol–glacial acetic acid and softened for 24 hr in 1 M NaOH at room temperature. They were stained overnight in 0.01% aniline blue in 0.15 M phosphate buffer, pH 10. Fluorescence was viewed by using a Leitz Ortholux II microscope (Wetzlar, Germany). Incident light was generated by a high-pressure mercury lamp passing through a UV UG1 excitation filter, and fluorescence was screened through a blue TK400 dichroic beam-splitting mirror.

In situ hybridizations were performed as described by Bowman et al. (1993). A 700-bp ClaI fragment of *ANT* cDNA5 extending to the 5′ end (Figure 4) was subcloned and used as a probe. This probe lacks conserved AP2 domains that may cross-hybridize with other non-*ANT* sequences. It was labeled as an antisense transcript with ^{35}S-UTP and hybridized with 8-μm serial sections of paraffin-embedded material. Slides were dipped in liquid emulsion (LM-1; Amersham), exposed for 8 to 12 days, developed with Kodak D19, and lightly stained with toluidine blue.

ACKNOWLEDGMENTS

We thank Bob Fischer for communicating unpublished results on *ANT* gene structure and for agreeing to coordinate publication, and we also thank Chuck Gasser for providing us with *ant-5* seed for an allelism test. We are grateful to Stan Alvarez for assistance in genetic manipulations and microscopy, Maria Moran for constructing the genomic library, Detlef Weigel for providing the cDNA library, John Bowman for his key help with the in situ hybridization experiments, and Hajime Sakai and Elliot Meyerowitz for communicating *SUP* results before publication. We particularly thank Stan Alvarez, Gerd Bossinger, John Bowman, Megan Griffith, Marcus Heisler, and Cameron Johnson for critical discussions, encouragement, and comments on the manuscript. This work was supported by Gene Shears Pty. Ltd. and the Australian Research Council (Grant No. A19230662 to D.R.S.).

Received October 30, 1995; accepted December 8, 1995.

REFERENCES

Angenent, G.C., Franken, J., Busscher, M., van Djiken, A., van Went, J.L., Dons, H.J.M., and van Tunen, A.J. (1995). A novel class of MADS box genes is involved in ovule development in petunia. Plant Cell **7**, 1569–1582.

Bouman, F. (1984). The ovule. In Embryology of the Angiosperms, B.M. Johri, ed (New York: Springer-Verlag), pp. 123–157.

Bowman, J.L., Smyth, D.R., and Meyerowitz, E.M. (1989). Genes directing flower development in *Arabidopsis*. Plant Cell **1**, 37–52.

Bowman, J.L., Drews, G.N., and Meyerowitz, E.M. (1991a). Expression of the Arabidopsis floral homeotic gene *AGAMOUS* is restricted to specific cell types late in flower development. Plant Cell **3**, 749–758.

Bowman, J.L., Smyth, D.R., and Meyerowitz, E.M. (1991b). Genetic interactions among floral homeotic genes of *Arabidopsis*. Development **112**, 1–20.

Bowman, J.L., Alvarez, J., Weigel, D., Meyerowitz, E.M., and Smyth, D.R. (1993). Control of flower development in *Arabidopsis thaliana* by *APETALA1* and interacting genes. Development **119**, 721–743.

Drews, G.N., Bowman, J.L., and Meyerowitz, E.M. (1991). Negative regulation of the Arabidopsis homeotic gene *AGAMOUS* by the *APETALA2* product. Cell **65**, 991–1002.

Finnegan, E.J., Lawrence, G.J., Dennis, E.S., and Ellis, J.G. (1993). Behavior of modified *Ac* element in flax callus and regenerated plants. Plant Mol. Biol. **22**, 625–633.

Gaiser, J.C., Robinson-Beers, K., and Gasser, C.S. (1995). The Arabidopsis *SUPERMAN* gene mediates asymmetric growth of the outer integuments of ovules. Plant Cell **7**, 333–345.

Herr, J.M., Jr. (1995). The origin of the ovule. Am. J. Bot. **82**, 547–564.

Hülskamp, M., Schneitz, K., and Pruitt, R.E. (1995). Genetic evidence for a long-range activity that directs pollen tube guidance in Arabidopsis. Plant Cell **7**, 57–64.

Jackson, D., Veit, B., and Hake, S. (1994). Expression of maize *KNOTTED1* related homeobox genes in the shoot apical meristem predicts patterns of morphogenesis in the vegetative shoot. Development **120**, 405–413.

Jofuku, K.D., den Boer, B.G.W., Van Montagu, M., and Okamuro, J.K. (1994). Control of Arabidopsis flower and seed development by the homeotic gene *APETALA2*. Plant Cell **6**, 1211–1225.

Kapil, R.N., and Tiwari, S.C. (1978). Plant embryological investigations and fluorescence microscopy: An assessment of integration. Int. Rev. Cytol. **53**, 291–331.

Lang, J.D., Ray, S., and Ray, A. (1994). *sin1*, a mutation affecting female fertility in *Arabidopsis*, interacts with *mod1*, its recessive modifier. Genetics **137**, 1101–1110.

Léon-Kloosterziel, K.M., Keijzer, C.J., and Koornneef, M. (1994). A seed shape mutant of Arabidopsis that is affected in integument development. Plant Cell **6**, 385–392.

Liu, Z., and Meyerowitz, E.M. (1995). *LEUNIG* regulates *AGAMOUS* expression in *Arabidopsis* flowers. Development **121**, 975–991.

Mitchell, P.J., and Tjian, R. (1989). Transcriptional regulation in mammalian cells by sequence-specific DNA binding proteins. Science **245**, 371–378.

Mizukami, Y., and Ma, H. (1995). Separation of *AG* function in floral meristem determinacy from that in reproductive organ identity by expressing antisense *AG* RNA. Plant Mol. Biol. **28**, 767–784.

Modrusan, Z., Reiser, L., Feldmann, K.A., Fischer, R.L., and Haughn, G.W. (1994). Homeotic transformation of ovules into carpel-like structures in Arabidopsis. Plant Cell **6**, 333–349.

Ochman, H., Medhora, M.M., Garza, D., and Hartl, D.L. (1990). Amplification of flanking sequences by inverse PCR. In PCR Protocol: A Guide to Methods and Applications, M.A. Innes, D.H. Gelfard, J.J. Sninsky, and T.J. White, eds (New York: Academic Press), pp. 219–227.

Ohme-Takagi, M., and Shinshi, H. (1995). Ethylene-inducible DNA binding proteins that interact with an ethylene-responsive element. Plant Cell **7**, 173–182.

Ray, A., Robinson-Beers, K., Ray, S., Baker, S.C., Lang, J.D., Preuss, D., Milligan, S.B., and Gasser, C.S. (1994). The *Arabidopsis* floral homeotic gene *BELL* controls ovule development through negative regulation of *AGAMOUS*. Proc. Natl. Acad. Sci. USA **91**, 5761–5765.

Reiser, L., and Fischer, R.L. (1993). The ovule and the embryo sac. Plant Cell **5**, 1291–1301.

Robinson-Beers, K., Pruitt, R.E., and Gasser, C.S. (1992). Ovule development in wild-type Arabidopsis and two female-sterile mutants. Plant Cell **4**, 1237–1249.

Rounsley, S.D., Ditta, G.S., and Yanofsky, M.F. (1995). Diverse roles for MADS box genes in Arabidopsis development. Plant Cell **7**, 1259–1269.

Sakai, H., Medrano, L.J., and Meyerowitz, E.M. (1995). Role of *SUPERMAN* in maintaining *Arabidopsis* floral whorl boundaries. Nature **378**, 199–203.

Schneitz, K., Hülskamp, M., and Pruitt, R.E. (1995). Wild-type ovule development in *Arabidopsis thaliana*: A light microscope study of cleared whole-mount tissue. Plant J. **7**, 731–749.

Sieburth, L.E., Running, M.P., and Meyerowitz, E.M. (1995). Genetic separation of third and fourth whorl functions of *AGAMOUS*. Plant Cell **7**, 1249–1258.

Smyth, D.R., Bowman, J.L., and Meyerowitz, E.M. (1990). Early flower development in *Arabidopsis*. Plant Cell **2**, 755–767.

Valvekens, D., Van Montagu, M., and Van Lijsebettens, M. (1988). *Agrobacterium tumefaciens*–mediated transformation of *Arabidopsis* root explants using kanamycin selection. Proc. Natl. Acad. Sci. USA **85**, 5536–5540.

Weigel, D. (1995). The APETALA2 domain is related to a novel type of DNA binding domain. Plant Cell **7**, 388–389.

Weigel, D., and Meyerowitz, E.M. (1994). The ABCs of floral homeotic genes. Cell **78**, 203–209.

Zhang, X.S., and O'Neill, S.D. (1993). Ovary and gametophyte development are coordinately regulated by auxin and ethylene following pollination. Plant Cell **5**, 403–418.